Nanoscale

Dynamic Article Links

Cite this: *Nanoscale*, 2011, **3**, 4427

www.rsc.org/nanoscale

PAPER

Enhanced near band edge luminescence of Ti/ZnO nanorod heterostructures due to the surface diffusion of Ti

Moumita Mahanti, Tushar Ghosh and Durga Basak*

Received 26th July 2011, Accepted 24th August 2011
DOI: 10.1039/c1nr10937e

Information on the mechanistic differences in the luminescence properties of Ti/ZnO nanorods (NRs) has been obtained through the preparation of heterostructures by (a) varying the thickness of Ti from 1 nm to 20 nm keeping the substrate temperature at 400 °C, (b) varying the substrate temperature from room temperature (RT) to 500 °C while keeping the metal thickness constant at 10 nm and (c) annealing the RT Ti sputtered NRs at temperatures of 400 °C and 500 °C. The photoluminescence (PL) spectra show that the near band edge luminescence of ZnO in the ultraviolet (UV) region is enhanced as the thickness of Ti increases up to 5 nm and, thereafter, it falls. Sputtering of Ti on ZnO NRs at RT does not cause any UV enhancement but when sputtered at and above 400 °C, the UV intensity is enhanced. Annealing of RT Ti sputtered NRs at and above 400 °C also results in the enhancement of the UV peak, although with a lesser magnitude. Analysis of the PL results, supported by X-ray diffraction, field emission scanning electron microscopy, elemental mapping, high resolution transmission electron microscopy, Fourier transform infrared spectroscopy and electrical *I–V* measurement results, show a clear indication that the surface diffusion of Ti causes a reduction in the surface defects.

Introduction

Over the past decades, ZnO has received tremendous attention because of its excellent material characteristics, such as a wide and direct band gap (3.37 eV) at room temperature (RT), a large exciton binding energy (60 meV), transparent conductivity, nontoxicity, *etc*.[1–4] In particular, being an excellent ultraviolet (UV) emitter and absorber, one dimensional (1D) ZnO nanostructures, such as nanowires (NWs) and nanorods (NRs), have received great attention in the past decade due to their potential applications in light emitting devices, as lasers or photodetectors[5–8] and their photocatalytic applications.[9,10] In general, the typical RT photoluminescence (PL) spectrum of ZnO shows a relatively sharp near band edge (NBE) emission in the UV region and a broad deep level emission (DLE) in the visible green/yellow/red region. The DLE in the green region is assigned to the oxygen vacancies (V_O) and/or zinc interstitials (Zn_i).[11–13] There are reports claiming that the visible emission is as a result of Li ion incorporation in the crystal,[14] while some report that an impurity, like a Cu ion, is responsible for the green emission.[15,16] Whatever the origin, the presence of a strong DLE emission indicates that a substantial amount of radiative recombinations occur *via* the deep defect centers, implying that any reduction in the DLE should augment the UV emission. The enhancement in the NBE in terms of the UV-to-Vis emission intensity ratio has therefore become one of the vital issues in the research of ZnO for its potential applications in the field of short wavelength semiconductor lasers and light emitting diodes.[17–19] Numerous efforts have focused on suppressing the visible emission by post-growth treatments, which include thermal annealing, plasma treatment, metallization, surface passivation and hydrogen treatment.[20–24] Much effort has been focused on the area of improved UV emission of ZnO thin films and nanostructures using metal capping since Okamoto *et al.*[25] first demonstrated the dramatic emission enhancement from the Ag-capped InGaN/GaN quantum well in 2004. The reason behind the emission enhancement is explained on the basis of surface plasmon (SP) resonance arising due to the local electric field enhancement near the surface of the metal nanoparticles and alteration of the radiative and non-radiative decay rates of the capped fluorescent materials.[26,27] There are several reports on enhanced PL emission due to different metal caps, such as Zn, Ag, Ni, Au, Al and Ti.[28–33] Among these, Au has been a popular choice to enhance the band gap luminescence[30–33] of ZnO, similar to many other semiconductor systems.[34–37] In most cases, the enhancement in luminescence has been explained on the basis of the coupling of light from ZnO with the surface plasmons of the metal caps.[29] The luminescence properties of ZnO are useful in the biomedical detection of drug carriers and in imaging diagnosis.[37] Au coated ZnO nanostructures could be a possible solution in obtaining stable and intensely luminescent nontoxic materials. However, although Au enhances the emission properties, it is costly. Since

Department of Solid State Physics, Indian Association for the Cultivation of Science, Jadavpur, Kolkata, 700032, India. E-mail: sspdb@iacs.res.in; Fax: +91 (33) 24732805

Ti is absolutely inert in the human body and a less costly metal, Ti coated ZnO nanostructures could be an alternative for Au/ZnO and thus the luminescence properties of Ti/ZnO heterostructures are worthy of investigation. However, when Ti has been used previously as a capping metal in ZnO films[38] as well as nanostructures,[17,39] it has been found that the film is doped with Ti at a temperature of 300 °C,[38] while the surface of the nanostructures becomes passivated by the metal layer at RT. On the other hand, Song *et al.*[39] have found that both SP coupling and surface passivation influence the enhancement of the UV emission in Ti-capped ZnO nanofibers, films and nanoparticles. Because of these contradictory statements in the literature, it is necessary to know the exact mechanism behind the change in the emission properties when Ti metal capping is used for ZnO nanostructures, especially since Ti is a reactive metal and popularly used as an n-type contact for ZnO.[40–42] Towards this goal, we aim to study the optical and electrical properties of Ti/ZnO NR heterostructures. For a detailed investigation, three series of samples have been prepared by varying (i) the thickness of the sputtered Ti layer, (ii) the substrate temperature during Ti sputtering and (iii) the post-sputtering annealing of Ti/ZnO NRs at different temperatures. We have found interesting results from which we have concluded that it is not surface plasmon resonance (SPR) coupling, but rather a surface diffusion mechanism passivating the surface defects of the NRs, which is responsible for the enhanced luminescence properties of Ti/ZnO NRs.

Experimental method

The ZnO NRs were first grown by an aqueous chemical (ACG) method on pre-cleaned glass substrates. The precursor materials were zinc acetate-2-hydrate [$Zn(CH_3COO)_2 \cdot 2H_2O$] (Sigma Aldrich, 99.999%) and hexamethylenetetramine [$(CH_2)_6N_4$] (Merck, 99.5%). The detailed growth procedure has been described elsewhere.[43,44] The ZnO NR arrays grown on the glass substrate were then loaded into a DC magnetron sputtering chamber. Ti was sputtered from a Ti metal target of purity 99.99% (MTI Corporation, USA) at a DC power of 50 W after a base pressure of 3.4×10^{-6} Torr was achieved. The substrate temperature was fixed at 400 °C while the metal thicknesses were varied (1, 3, 5, 10, 15 and 20 nm) for the 1st series of samples (series A). The thickness was estimated from an optimized thickness monitor fitted inside the sputtering chamber. By keeping the thickness of the Ti layer constant at 10 nm, the substrate temperature was varied at 200 °C, 300 °C, 400 °C, and 500 °C for the 2nd series of samples (series B). After Ti sputtering, the samples were first cooled down to RT under a high vacuum and then taken out of the chamber to avoid any oxidation of the Ti. We also sputtered Ti (10 nm) at RT on the NRs, which were then annealed at 400 °C and 500 °C for 45 min in an inert atmosphere of Ar to prepare the 3rd series of samples (series C). The PL spectra at RT were measured using a He–Cd laser (Kimmon Koha Co., Ltd.; model KR1801C) with a 325 nm excitation source and recording of the luminescence using a spectrometer (Horiba Jobin Yvon, Model: iHR 320) together with a photomultiplier tube. Investigations of the crystalline phase and morphology were carried by X-ray diffractometer (XRD, model Seifert XDAL 3000), field emission scanning electron microscopy (FESEM, model JEOL JSM-6700F) and high-resolution transmission electron microscopy (HRTEM, model JEM 2010). The elemental mapping was also done using the same FESEM system. Fourier transform infrared (FTIR) spectroscopy (Shimadzu model FTIR-8400) was done in the wavenumber region between 400 and 4000 cm^{-1}.

Results and discussion

Room temperature PL spectra of Ti-coated ZnO NRs for series A samples are shown in Fig. 1. The photoluminescence spectrum of the pristine ZnO NRs shows a strong UV emission at 380 nm due to exciton recombination and a broad visible emission ranging from 400–700 nm, which is attributed to defect-related radiative recombination. There is no significant change in the visible emission due to Ti sputtering under the present experimental conditions. Therefore, we only concentrate on the changes in the UV emission. As the thickness of the sputtered Ti layer increases, the UV emission intensity increases (Fig. 1). For a 5 nm layer of Ti, the UV emission intensity becomes about five times larger than that of the pristine NRs. With an increase in thickness beyond 5 nm, the intensity gradually falls and finally becomes smaller than that of the pristine NRs for a 20 nm Ti coating. Since the pumping power and focusing conditions of the excitation source are kept similar during the PL measurements, the observed change in the PL intensity for the different samples can be assigned to the change in the crystalline properties of the NRs. Fig. 2 shows the PL spectra of samples from series B. It shows that when Ti is sputtered on ZnO NRs at RT, there is no enhancement in the UV intensity, instead the emission intensity is lower than that of the pristine NRs. This is in contrast to the results of Song *et al.*,[39] where the UV emission intensity was enhanced by Ti sputtering at RT. As the substrate temperature increases in our case, the intensity of the UV emission also increases. The results shown in Fig. 1 and 2 indicate that the substrate temperature during Ti sputtering plays a crucial role in the UV emission intensity. In order to know if the substrate temperature really plays a key role or not, samples from series C have been prepared by annealing the Ti/ZnO heterostructures (where Ti is sputtered on the NRs at RT) at 400 °C and 500 °C in an inert atmosphere (Ar) and their PL spectra have been

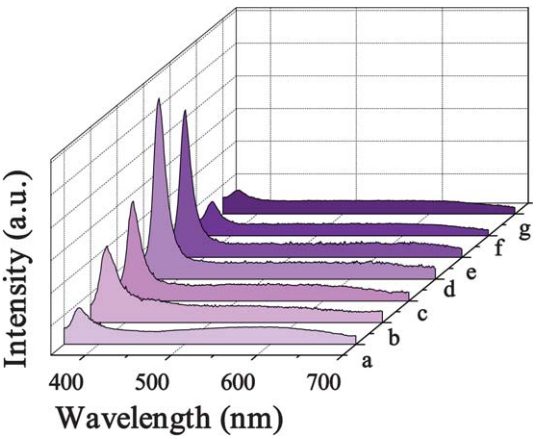

Fig. 1 Room temperature PL spectra of (a) pristine ZnO NRs and Ti/ZnO NR heterostructures for Ti (b) 1 nm, (c) 3 nm, (d) 5 nm, (e) 10 nm, (f) 15 nm, (g) 20 nm.

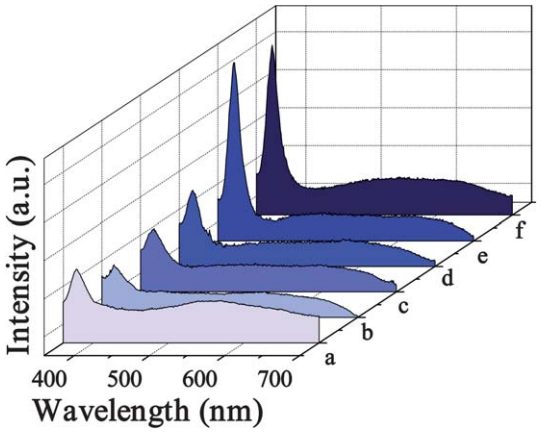

Fig. 2 Room temperature PL spectra of (a) pristine ZnO NRs and Ti/ZnO NR heterostructures for Ti (10 nm) sputtered at (b) room temperature, (c) 200 °C, (d) 300 °C, (e) 400 °C, (f) 500 °C.

recorded as shown in Fig. 3. This shows that the UV emission intensity increases upon annealing and becomes about 1.6 and 2 times that of the pristine NRs following annealing at 400 °C and 500 °C, respectively. This enhancement in the values is, however, less than when the substrate temperatures were 400 °C and 500 °C. Thus, these results indicate that a supply of thermal energy during sputtering affects the UV emission much more than the changes resulting from the supply of the same thermal energy during post-sputtering annealing. To ascertain that the enhancement in the UV emission is not due to treatment of the pristine NRs with a similar Ar plasma or annealing at a higher temperature, two pristine control samples have been prepared under identical conditions to those used to prepare NR heterostructures, one each from series B and series C, which showed the highest UV emission. The PL spectra in Fig. 4 show that when the pristine NRs are treated with Ar plasma at a higher temperature, there is an enhancement in their UV emission, similar to the reports of Dev *et al.*[23]. However, the observed enhancement is only 1.5 times as compared to 5 times when only Ti coating is done (Fig. 4). When the pristine NRs are annealed at 500 °C, the UV emission intensity is quenched and the visible

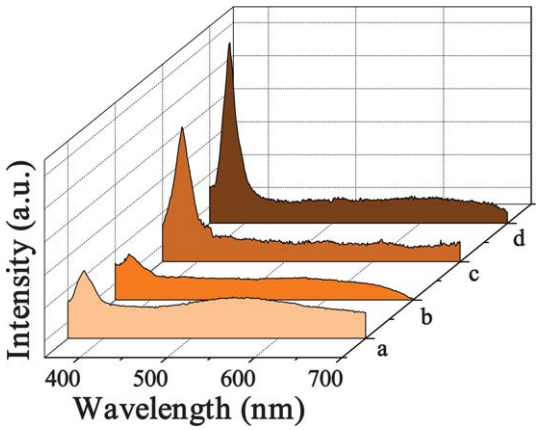

Fig. 3 Room temperature PL spectra of (a) pristine ZnO NRs and Ti/ZnO NR heterostructures for Ti (10 nm) sputtered at (b) room temperature and annealed at (c) 400 °C and (d) 500 °C.

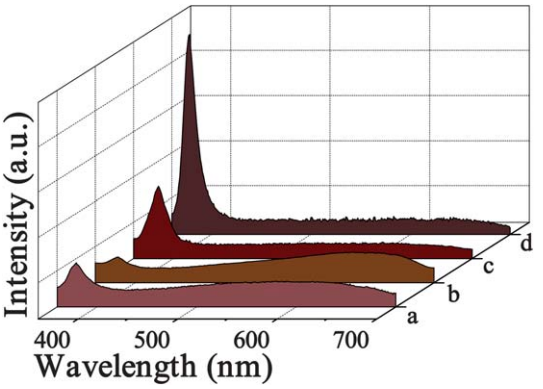

Fig. 4 Room temperature PL spectra of (a) pristine ZnO NRs, (b) ZnO NRs annealed at 500 °C, (c) ZnO NRs treated with Ar plasma at 400 °C and (d) Ti/ZnO NR heterostructures for Ti (10 nm) sputtered at 400 °C.

emission is enhanced, similar to earlier observations.[45] These results confirm that such large changes in the UV emission are due to coating with Ti under particular conditions. The PL results, therefore, support our proposition that it is the temperature of the NRs during Ti sputtering that plays a key role in the changing of the emission properties.

In general, an emission energy from the semiconductor, which matches quite closely the SP energy of the metal, can induce a larger enhancement in the spontaneous recombination rate due to a strong resonant coupling effect.[25,46] The resonance energies of the surface plasmons can be calculated using the dispersion relation (1):[47]

$$\hbar k_{sp} = \frac{\hbar\omega}{c}\sqrt{\frac{\varepsilon_{ZnO}\varepsilon_m}{\varepsilon_{ZnO}+\varepsilon_m}} \quad (1)$$

where k_{sp} is the wave vector of the surface plasmon, ε_m and ε_{ZnO} are the dielectric constants of the metal and ZnO,[48,49] respectively, and $\hbar\omega$ is the incident energy. The surface plasmon energy of Ag/ZnO is found to be 2.93 eV, which indicates that the right combination of metal and semiconductor may lead to a SPR coupling of the NBE emission from the metal.[46] On the other hand, a fair match between the SPR coupling energy of Au nanoparticles and the defect emissions of ZnO results in an enhancement of the defect emission.[50] While, for Ti/ZnO system, the SPR energy is above 10 eV as the dielectric constant of Ti metal is much higher than that of ZnO.[39] The value is far away from the emission energies of ZnO. In addition, the separation distance between the semiconductor and the metal has been found to play a very important role in determining the extent of the PL enhancement and quenching.[35,51,52] Since, in the present study, similar NRs (grown under identical conditions) have been used for all the metal sputtering experiments, the distance between the metal and the semiconductor surface can be regarded as constant, which rules out the possibility of any enhancement due to the distance effect. Therefore, the observed UV enhancement in our sample can not be assigned to the SP coupling. Our proposition is supported further by the fact that the UV emission is not enhanced when 10 nm Ti is sputtered on the NRs at RT. Song *et al.*[39] proposed that a surface passivation mechanism, in addition to SP coupling, is responsible for the UV enhancement, although they did mention at the same time that

the SP coupling energy is much larger than that of ZnO emissions. Thus, as a reasonable cause of the enhanced emission, we may consider two other possibilities: (i) surface modification and (ii) surface diffusion. If surface modification was the cause of the UV enhancement, there would also be some enhancement when Ti was sputtered at and below 300 °C, including RT. But in these cases, no enhancement, as compared to the pristine NRs, has been found (Fig. 2 and Fig. 3). Thus, the possibility of surface modification as a reason for the UV enhancement can be ruled out. Now, let us check the feasibility of diffusion. Diffusion in solids in general takes an extensively long reaction time. Usually, the slow diffusion rates can be overcome by using higher reaction (substrate) temperatures as well as using more active (plasma generated) and energetic (magnetron generated) species. Our results indicate that when Ti is sputtered on ZnO NRs at higher substrate temperatures, Ti diffusion into the ZnO surface lattice occurs due to the impingement of high energy Ti species (ions and radicals) on to the NRs, which is assisted by the thermal energy supplied to the NRs. With the ionic radius of stable Ti^{4+} (74.5 pm) being less than that of Zn^{2+} (88 pm),[53] the former can occupy the position of Zn easily. The absence of an appreciable thermal energy causes no Ti diffusion, as can be derived from Fig. 2. Due to the inherent nature of the surface, there exist abundant defects. V_{Zn} defects are known to exist on the surface of the NRs, which has been confirmed by different experiments, like positron annihilation spectroscopy, HRTEM and X-ray adsorption fine structure studies, as well as first principle calculations.[54–59] However, we could not show the existence of V_{Zn} directly at the moment. Diffused Ti is more likely to occupy these vacant Zn sites and, thereby, cause a reduction in surface defects. It is well known that surface defects are presumed to be the preferential channels of charge carrier recombination, which can inhibit NBE emission. Therefore, any reduction of these recombination centres would enhance the UV emission.[60,61] There are a couple of studies on the Ti/ZnO system: Lu *et al.* have shown Ti diffusion on the surface of ZnO,[38] while Chang *et al.* have assigned the occupation of Ti in Zn sites in the ZnO lattice when the NWs were implanted with Ti beams.[62] Lu *et al.*[38] have also reported that when Ti is deposited on ZnO, an interfacial reaction occurs between Ti and ZnO and, consequently, a significant amount of Zn moves to the surfaces after post annealing at 400 °C. Therefore, one may argue at this stage that Ti in the present study may also form its oxide by reacting with the oxygen. However, we have not observed any peak of either Ti or TiO_2 in the XRD patterns of the series B samples, where Ti is sputtered at 400 °C or 500 °C (Fig. 5). On the other hand, a reaction with oxygen is evident from the presence of a TiO_2 phase in the XRD patterns of the series C samples when the heterostructure is annealed at 400 °C and 500 °C (Fig. 5). Since Ti has a stronger tendency to react with oxygen than Zn, it is expected that when the Ti/ZnO heterostructure is annealed at higher temperatures, Ti would react with the interfacial oxygen atoms leaving free Zn, which may then migrate to the surface.[38] A comparison of the full width at half maximum (FWHM) for the (002) peak of the Ti/ZnO NR heterostructures with that of the pristine NRs (Fig. 5) also confirms that there is only a slight improvement (probably due to a reduction in the surface defects) in the crystal quality as a result of Ti sputtering at a higher temperature. However, post-sputtering annealing leads to

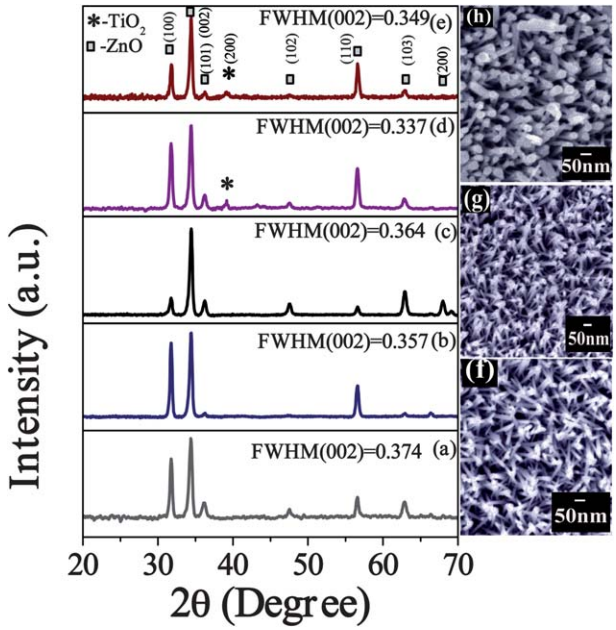

Fig. 5 XRD spectra of (a) pristine ZnO NRs and Ti/ZnO NR heterostructures for Ti (10 nm) sputtered at (b) 400 °C, (c) 500 °C, and Ti (10 nm) sputtered at room temperature and annealed at (d) 400 °C and (e) 500 °C. FESEM images of (f) pristine ZnO NRs, (g) Ti/ZnO NR heterostructures for Ti (10 nm) sputtered at 400 °C and (h) Ti/ZnO NR heterostructures for Ti (10 nm) sputtered at room temperature and annealed at 400 °C.

a much better crystal quality as evident from the significant change in the FWHM values (Fig. 5). As the UV emission increases with an increase either in the thickness of Ti or the substrate temperature (Fig. 1 and Fig. 2), diffusion of more Ti to the NR's surface is indicated. A closer look at the morphology of the NRs in the FESEM images, shown in Fig. 5, reveals that both the pristine ZnO NRs and the sample from series B have a comparable NR diameter, while the sample from series C has a slightly larger diameter. This is expected if there is an interfacial reaction product (TiO_2). In order to confirm the presence of Ti, elemental mapping from an area of the NR (series B, 400 °C) has been performed and is shown in Fig. 6. Uniformly distributed signals from Ti can be seen in the entire area, confirming the presence of Ti along the entire length of the NR. This signal from Ti is not only originating from the surface of the NR, but may also come from the bulk as the penetration depth of the electrons in the energy-dispersive X-ray spectroscopy (EDS) analysis was >15 nm, as calculated from the beam current and voltage. TEM and HRTEM studies (Fig. 7) also show the clear presence of a Ti layer in a RT sputtered NR (series B). On the other hand, the HRTEM image of the NR (series B, 400 °C) shows only a very thin layer of Ti around the ZnO NR's surface. In both cases, the sputtered Ti layer was 10 nm thick (as estimated from the thickness monitor in the chamber); however, the Ti layer is only ~4 nm thick when the substrate temperature was 400 °C and ~9 nm when it was at RT. Combining the results obtained from Fig. 6 and Fig. 7, it can be inferred that a certain amount of Ti is diffused into the lattice sites. However, the lattice fringes observed in Fig. 7 correspond to only the $\{10\bar{1}1\}$ plane of the ZnO wurtzite structure.[44] Therefore, it is probable that the

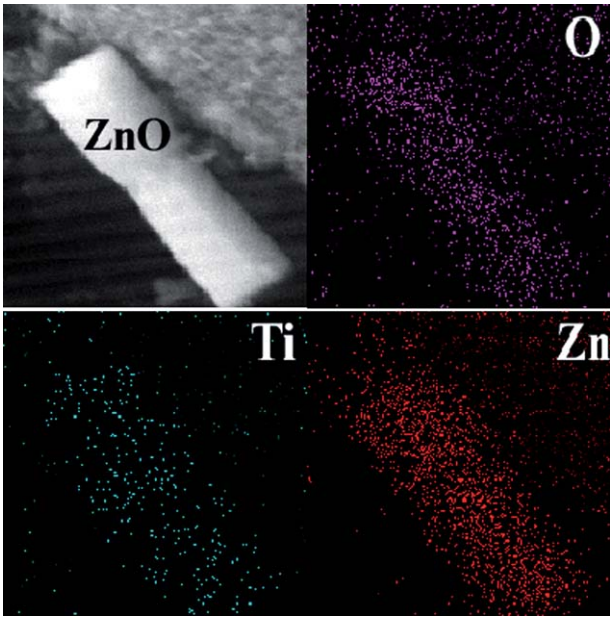

Fig. 6 Elemental mapping of Ti/ZnO NR heterostructures for Ti (10 nm) sputtered at 400 °C.

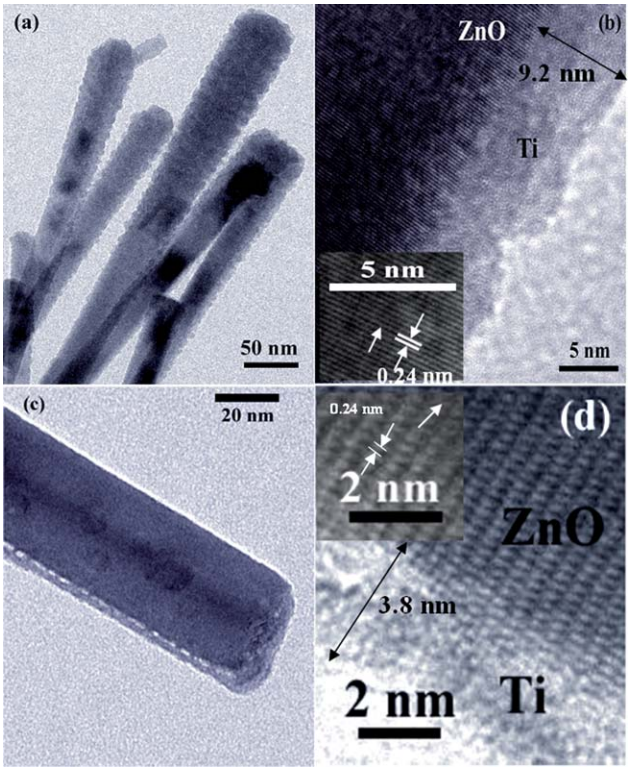

Fig. 7 (a) TEM and (b) HRTEM images of Ti/ZnO NR heterostructures for Ti (10 nm) sputtered at room temperature, and (c) TEM and (d) HRTEM images of Ti/ZnO NR heterostructures for Ti (10 nm) sputtered at 400 °C.

sputtered Ti is amorphous in nature and, thus, we have neither found any Ti peak in the XRD pattern (Fig. 5) nor any other lattice fringes in the HRTEM images (Fig. 7). These results clearly indicate Ti diffusion on to the ZnO NR's surface. Ti

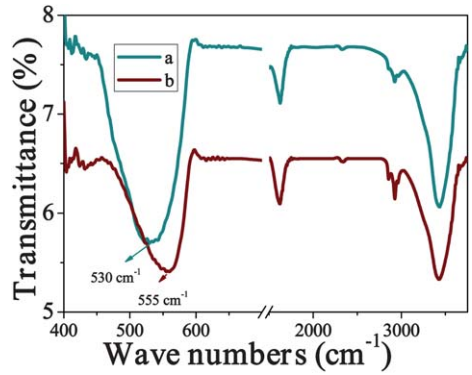

Fig. 8 FTIR spectra of pristine ZnO NRs (a) and Ti/ZnO NR heterostructures for Ti (10 nm) sputtered at 400 °C (b).

diffusion is further confirmed by the FTIR results shown in Fig. 8. It shows that the frequency of the Zn–O vibrational mode at 530 cm^{-1} for the pristine NRs[63] is shifted to a higher frequency region at 555 cm^{-1} for the Ti/ZnO heterostructure, indicating the possible occupation of the Zn sites by Ti. Ti diffusion to the surfaces of the ZnO NRs can be explained by the models shown in Fig. 9.

The diffusion of Ti is also suggested by the electrical *I–V* measurements. Fig. 10(I) shows that when Ti is sputtered at higher temperatures, such as 400 °C and 500 °C (all are not shown), the current level increases appreciably, as compared to the pristine NRs when Ti is sputtered at RT and subsequently annealed at higher temperatures of 400 and 500 °C. Interestingly, the current magnitudes in the case of the annealed samples are lower than those when Ti is sputtered at 400 and 500 °C. Fig. 10 (II) shows that the current level also increases in case of the control NR samples treated under similar Ar plasma and post-sputtering annealing conditions, but the increase is much lower compared to the high temperature sputtered samples. The

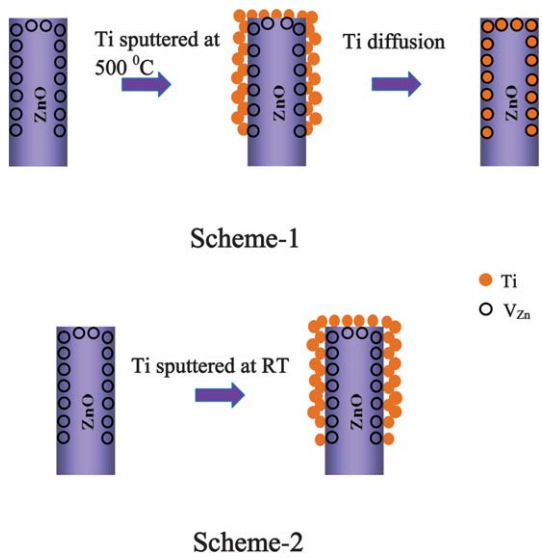

Fig. 9 The proposed models for Ti/ZnO NR heterostructures for (Scheme-1) Ti sputtering and diffusion at 500 °C and (Scheme-2) Ti sputtering at room temperature.

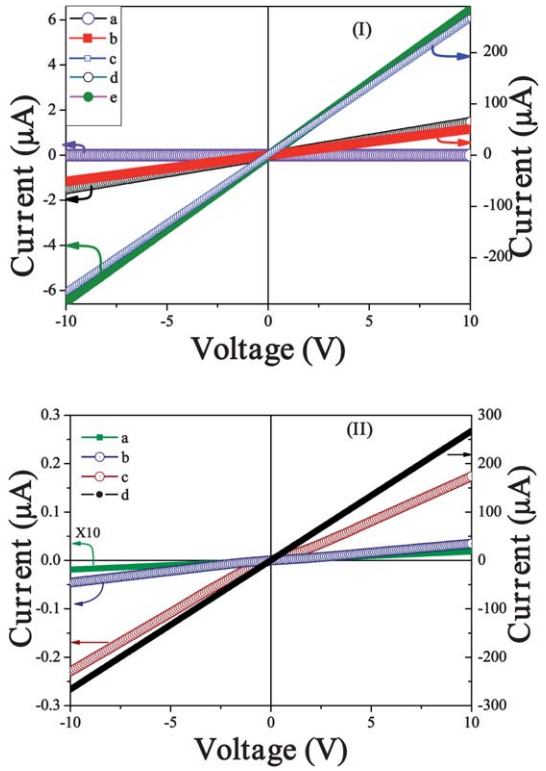

Fig. 10 **(I)** Schematic diagram of *I–V* measurements for (a) pristine ZnO NRs and Ti/ZnO NR heterostructures for Ti (10 nm) sputtered at (b) 400 °C and (c) 500 °C, Ti sputtered at room temperature and annealed at (d) 400 °C and (e) 500 °C. **(II)** Schematic diagram of *I–V* measurements of (a) pristine ZnO NRs, (b) ZnO NRs annealed at 500 °C, (c) ZnO NRs treated with Ar plasma at 400 °C and (d) Ti/ZnO NR heterostructures for Ti (10 nm) sputtered at 400 °C.

increase in the current magnitude is due to an increase in the number of free carriers owing to the extra electrons lost by the Ti ions (in the case of surface diffusion). A reduction in the surface trap states causes an increase in the current conduction in the case of the annealed samples. The results are in good agreement with the PL and XRD results.

Conclusions

In conclusion, the luminescence properties of Ti/ZnO NR heterostructures prepared by varying the Ti layer thickness, substrate and post-sputtering annealing temperatures, have been investigated. The NBE luminescence is enhanced 5 times when Ti is sputtered on the NRs at 400 °C. There is no enhanced UV emission when Ti is sputtered at RT. By examining the dependence of the enhancement on the substrate and annealing temperature and the structure and microstructure of the Ti/ZnO NRs, our results can be well explained on the basis of Ti surface diffusion when the latter is sputtered at and above 400 °C. These studies are very useful for the design of highly UV emitting nanostructures for emitter applications. In addition, with Ti being the most biocompatible metal among all the metals, our results indicate that this is an attractive approach for the application of Ti/ZnO systems in biomedical fields.

Acknowledgements

The authors are thankful to DAE-BRNS for the financial support of this work *via* project 2009/37/21/BRNS/1097.

References

1 R. F. Oulton, V. J. Sorger, T. Zentgraf, R. M. Ma, C. Gladden, L. Dai, G. Bartal and X. Zhang, *Nature*, 2009, **461**, 629.
2 Z. L. Wang and J. Song, *Science*, 2006, **312**, 242.
3 A. L. Briseno, T. W. Holcombe, A. I. Boukai, E. C. Garnett, S. W. Shelton, J. J. M. Frchet and P. Yang, *Nano Lett.*, 2010, **10**, 334.
4 J. M. Wu, Y.-R. Chen and Y.-H. Lin, *Nanoscale*, 2011, **3**, 1053.
5 J. S. Liu, C. X. Shan, B. H. Li, Z. Z. Zhang, C. L. Yang, D. Z. Shen and X. W. Fan, *Appl. Phys. Lett.*, 2010, **97**, 251102.
6 H. Zhu, C. X. Shan, L. K. Wang, Y. Yang, J. Y. Zhang, B. Yao, D. Z. Shen and X. W. Fan, *Appl. Phys. Lett.*, 2010, **96**, 041110.
7 C. Soci, A. Zhang, B. Xiang, S. A. Dayeh, D. P. R. Aplin, J. Park, X. Y. Bao, Y. H. Lo and D. Wang, *Nano Lett.*, 2007, **7**, 1003.
8 X. M. Zhang, M. Y. Lu, Y. Zhang, L. J. Chen and Z. L. Wang, *Adv. Mater.*, 2009, **21**, 2767.
9 D. Deng, S. T. Martin and S. Ramanathan, *Nanoscale*, 2010, **2**, 2685.
10 Z. Zhang, C. Shao, X. Li, C. Wang, M. Zhang and Y. Liu, *ACS Appl. Mater. Interfaces*, 2010, **2**, 2915.
11 K. Vanheusden, W. L. Warren, C. H. Seager, D. R. Tallant, J. A. Voigt and B. E. Gnade, *J. Appl. Phys.*, 1996, **79**, 7983.
12 M. Liu, A. H. Kitai and P. Mascher, *J. Lumin.*, 1992, **54**, 35.
13 Q. X. Zhao, P. Klason, M. Willander, H. M. Zhong, W. Lu and J. H. Yang, *Appl. Phys. Lett.*, 2005, **87**, 211912.
14 D. Li, Y. H. Leung, A. B. Djurišic, Z. T. Liu, M. H. Xie, S. L. Shi and S. J. Xu, *Appl. Phys. Lett.*, 2004, **85**, 1601.
15 Y. Liu, H. Liang, L. Xu, J. Zhao, J. Bian, Y. Luo, Y. Liu, W. Li, G. Wu and G. Du, *J. Appl. Phys.*, 2010, **108**, 113507.
16 N. C. Giles, N. Y. Garces, L. Wang and L. E. Halliburton, *Proc. SPIE–Int. Soc. Opt. Eng.*, 2004, **5359**, 267–278.
17 J. Dintinger, S. Klein and T. W. Ebbesen, *Adv. Mater.*, 2006, **18**, 1267.
18 M. H. Huang, S. Mao, H. Feick, H. Q. Yan, Y. Y. Wu, H. Kind, E. Weber, R. Russo and P. D. Yang, *Science*, 2001, **292**, 1897.
19 S. J. Pearton, D. P. Norton, K. Ip, Y. W. Heo and T. Steiner, *J. Vac. Sci. Technol., B*, 2004, **22**, 932.
20 C. X. Shan, Z. Liu and S. K. Hark, *Appl. Phys. Lett.*, 2008, **92**, 073103.
21 N. Ohashi, T. Ishigaki, N. Okada, H. Taguchi, I. Sakaguchi, S. Hishita, T. Sekiguchi and H. Haneda, *J. Appl. Phys.*, 2003, **93**, 6386–6392.
22 Y. M. Strzhemechny, J. Nemergut, P. E. Smith, J. Bae, D. C. Look and L. J. Brillson, *J. Appl. Phys.*, 2003, **94**, 4256–4262.
23 A. Dev, J. P. Richters, J. Sartor, H. Kalt, J. Gutowski and T. Voss, *Appl. Phys. Lett.*, 2011, **98**, 131111.
24 A. Dev, R. Niepelt, J. P. Richters, C. Ronning and T. Voss, *Nanotechnology*, 2010, **21**, 065709.
25 K. Okamoto, L. Niki, A. Shvartser, Y. Narukawa, T. Mukai and A. Scherer, *Nat. Mater.*, 2004, **3**, 601.
26 Z. Yang, W. Ni, X. Kou, S. Zhang, Z. Sun, L. D. Sun, J. Wang and C. H. Yan, *J. Phys. Chem. C*, 2008, **112**, 18895.
27 Z. H. Sun, Z. Yang, J. H. Zhou, M. H. Yeung, W. H. Ni, H. K. Wu and J. F. Wang, *Angew. Chem., Int. Ed.*, 2009, **48**, 2881–2885.
28 Y. J. Fang, J. Sha, Z. L. Wang, Y. T. Wan, W. W. Xia and Y. W. Wang, *Appl. Phys. Lett.*, 2011, **98**, 033103.
29 C. W. Cheng, E. J. Sie, B. Liu, C. H. A. Huan, T. C. Sum, H. D. Sun and H. J. Fan, *Appl. Phys. Lett.*, 2010, **96**, 071107.
30 M. K. Lee, T. G. Kim and Y. M. Sung, *J. Phys. Chem. C*, 2008, **112**, 10079–10082.
31 Y. K. Mishra, S. Mohapatra, R. Singhal, D. K. Avasthi, D. C. Agarwal and S. B. Ogale, *Appl. Phys. Lett.*, 2008, **92**, 043107.
32 X. Li, Y. Zhang and X. Ren, *Opt. Express*, 2009, **17**, 8735–8740.
33 V. Subramanian, E. E. Wolf and P. V. Kamat, *J. Phys. Chem. B*, 2003, **107**, 7479–7485.
34 H. Y. Lin, Y. F. Chen, J. G. Wu, D. I. Wang and C. C. Chen, *Appl. Phys. Lett.*, 2006, **88**, 161911.
35 C. W. Chen, C. H. Wang, C. M. Wei and Y. F. Chen, *Appl. Phys. Lett.*, 2009, **94**, 071906.

36 Z. Yang, W. H. Ni, X. S. Kou, S. Z. Zhang, Z. H. Sun, J. F. Wang and C. H. Yan, *J. Phys. Chem. C*, 2008, **112**, 18895–18903.
37 H. Xiong, Y. Xu, Q. Ren and Y. Xia, *J. Am. Chem. Soc.*, 2008, **130**, 7522; P. Zhang and W. Liu, *Biomaterials*, 2010, **31**, 3087.
38 J. J. Lu, Y. M. Lu, S. I. Tasi, T. L. Hsiung, H. P. Wang and L. Y. Jang, *Opt. Mater.*, 2007, **29**, 1548–1552.
39 J. Song, X. An, J. Zhou, Y. Liu, W. Wang, X. Li, W. Lan and E. Xie, *Appl. Phys. Lett.*, 2010, **97**, 122103.
40 H. K. Kim, S. H. Han, T. Y. Seong and W. K. Choi, *J. Electrochem. Soc.*, 2001, **148**, G114.
41 H. K. Kim, S. H. Han, T. Y. Seong and W. K. Choi, *Appl. Phys. Lett.*, 2000, **77**, 1647.
42 H. S. Yang, D. P. Norton and S. J. Pearton, *Appl. Phys. Lett.*, 2005, **87**, 212106.
43 A. Bera and D. Basak, *Appl. Phys. Lett.*, 2008, **93**, 053102.
44 S. Panigrahi and D. Basak, *Nanoscale*, 2011, **3**, 2336.
45 A. Bera and D. Basak, *Chem. Phys. Lett.*, 2009, **476**, 262–266.
46 C. W. Lai, J. An and H. C. Ong, *Appl. Phys. Lett.*, 2005, **86**, 251105.
47 W. L. Barnes, A. Dereux and T. W. Ebbesen, *Nature*, 2003, **424**, 824.
48 M. A. Ordal, R. J. Bell, J. R. W. Alexander, L. L. Long and M. R. Querry, *Appl. Opt.*, 1985, **24**, 4493.
49 P. L. Washington, H. C. Ong, J. Y. Dai and R. P. H. Chang, *Appl. Phys. Lett.*, 1998, **72**, 3261.
50 B. J. Niu, L. L. Wu, W. Tang, X. T. Zhang and Q. G. Meng, *CrystEngComm*, 2011, **13**, 3678.
51 O. Kulakovich, N. Strekal, A. Yaroshevich, S. Maskevich, S. Gaponenko, I. Nabiev, U. Woggon and M. Artemyev, *Nano Lett.*, 2002, **2**, 1449.
52 W. H. Ni, J. An, C. W. Lai, H. C. Ong and J. B. Xu, *J. Appl. Phys.*, 2006, **100**, 026103.
53 R. D. Shannon, *Acta Crystallogr., Sect. A: Cryst. Phys., Diffr., Theor. Gen. Crystallogr.*, 1976, **32**, 751–767.
54 I. Shalish, H. Temkin and V. Narayanamurti, *Phys. Rev. B: Condens. Matter Mater. Phys.*, 2004, **69**, 245401.
55 A. B. Djurisic and Y. H. Leung, *Small*, 2006, **2**, 944.
56 F. Tuomisto, V. Ranki, K. Sarrinen and D. C. Look, *Phys. Rev. Lett.*, 2003, **91**, 205502.
57 Y. Ding, R. Yang and Z. L. Wang, *Solid State Commun.*, 2006, **138**, 390.
58 W. Yan, Z. Sun, Q. Liu, Z. Li, Z. Pan, J. Wang, S. Wei, D. Wang, Y. Zhou and X. Zhang, *Appl. Phys. Lett.*, 2007, **91**, 062113.
59 A. F. Kohan, G. Ceder, D. Morgan and C. V. Van de Walle, *Phys. Rev. B: Condens. Matter*, 2000, **61**, 15019.
60 A. Bera, T. Ghosh and D. Basak, *ACS Appl. Mater. Interfaces*, 2010, **2**, 2898.
61 H. Y. Shih, Y. T. Chen, N. H. Huang, C. M. Wei and Y. F. Chen, *J. Appl. Phys.*, 2011, **109**, 103523.
62 W. Chang, Y. C. Sung, J. W. Yeh and H. C. Shih, *J. Appl. Phys.*, 2011, **109**, 074318.
63 F. J. Manjon, B. Marí, J. Serrano and A. H. Romero, *J. Appl. Phys.*, 2005, **97**, 053516.